LAND DEGRADATION & DEVELOPMENT
Land Degrad. Develop. **28**: 648–663 (2017)
Published online 26 August 2016 in Wiley Online Library (wileyonlinelibrary.com) **DOI**: 10.1002/ldr.2592

INTERACTION BETWEEN PLANT ROOTS AND SOIL WATER FLOW IN RESPONSE TO PREFERENTIAL FLOW PATHS IN NORTHERN CHINA

Yinghu Zhang[1], Jianzhi Niu[2]*, Mingxiang Zhang[1]*, Zixing Xiao[2], Weili Zhu[2]

[1]*School of Nature Conservation, Beijing Forestry University, Qinghua East Road 35, Beijing, Haidian District 100083, PR China*
[2]*Key Laboratory of Soil and Water Conservation and Desertification Combating, Ministry of Education, School of Soil and Water Conservation, Beijing Forestry University, Qinghua East Road 35, Beijing, Haidian District 100083, PR China*

Received 13 January 2016; Revised 21 July 2016; Accepted 22 July 2016

ABSTRACT

Preferential flow is expected to provide preferential channels for plant root growth and variations in soil water flow, but few studies were conducted to imply the impacts of these changes, particularly for preferential flow in stony soils. This study aimed to characterize soil water flow and plant root distribution in response to preferential flow paths and quantitatively describe the relation between plant root distribution and soil water flow. Field dye-tracing experiments centered on experimental plants were conducted to determine the root length density and soil water flow process. Laboratory analyses were performed to characterize changes in the relative concentration of the accumulated effluent and the degree of interaction between plant roots and soil water flow. The amount of fine plant roots with preferential flow paths decreased with increasing soil depth for all experimental plots. The largest plant roots were recorded in the upper soil layers to a depth of 20 cm. The relative concentration of the accumulated effluent increased with time and decreased with soil depth under saturated soil conditions, whereas a distinct early turning point for the relative concentration of the accumulated effluent was observed in the 0–20-cm soil columns, and the relative concentration of the accumulated effluent initially decreased and then increased with time under unsaturated soil conditions. This study provides quantitative information with which to characterize the interaction between plant roots and soil water flow in response to preferential flow paths in soil–plant–water systems. Copyright © 2016 John Wiley & Sons, Ltd.

KEY WORDS: preferential flow; soil matrix; fine plant roots; root length density; soil water content

INTRODUCTION

Serious environmental issues, including water crises, land degradation, urban agricultural food security, and air pollution, threaten the livelihoods of people worldwide (Alonso-Sarría *et al.,* 2016; Beniston *et al.,* 2016; Ni *et al.,* 2015; Singh *et al.,* 2015; Cerdà *et al.,* 2016; Keesstra *et al.,* 2016a). These environmental issues and other social, economic, geologic, and human health-related issues could be better addressed if the soil hydrological processes were more fully considered (Brevik *et al.,* 2015; Marchamalo *et al.,* 2016). The soil hydrological process, with preferential flow as one of the factors influencing environmental issues, specifically land degradation and groundwater resource security, occurs throughout the world and has been studied on different scales from field plot and hillslope scale to the catchment scale (Zehe *et al.,* 2010; Beven & Germann, 2013; Keesstra *et al.,* 2016b). A variety of materials in soils, including heavy metals, radionuclides, pesticides, and contaminants, cause environmental issues through preferential flow paths. Soils with a large number of preferential flow paths and more continuity of vertically oriented preferential flow paths promote water flow, and these flow paths change the soil hydrological process (Cerdà & Jurgensen, 2008; Cerdà *et al.,* 2009; De Boever *et al.,* 2014; Wang *et al.,* 2016).

Preferential flow encompasses situations in which water flow and solute transportation occur via preferential flow paths. This phenomenon occurs at a wide range of spatial and temporal scales, causing runoff to quickly bypass the surrounding soil matrix and reach groundwater level. Moreover, as a prevailing phenomenon in soil hydrological processes, preferential flow can promote water flow and solute transportation with little resistance (Bogner *et al.,* 2010). This phenomenon is critical to understanding the biogeocenotic and global ecological functions of soil, such as the loss of soil fertility and nutrients, the intense erodibility of topsoil, the low activity of soil microorganisms stemming from the intense use of fertilizers and pesticides, and the formation of chemical compositions in groundwater (Brevik *et al.,* 2015; Singh *et al.,* 2015). Therefore, understanding the land degradation response to preferential flow is essential (Cerdà, 1999).

Studies on the preferential flow response to plant roots and soil water flow, which tend to characterize land degradation, are hot spots in pedological research (Zhao *et al.,* 2016). Preferential flow as a highly random and unpredictable process results in complex flow patterns and leads to a huge pollution risk (Nimmo, 2012). Preferential flow at

*Correspondence to: J. Niu, Key Laboratory of Soil and Water Conservation and Desertification Combating, Ministry of Education, School of Soil and Water Conservation, Beijing Forestry University, Qinghua East Road 35, Beijing, Haidian District, 100083, PR China.
E-mail: yhzhang2015sd@bjfu.edu.cn
M. Zhang, School of Nature Conservation, Beijing Forestry University, Qinghua East Road 35, Beijing, Haidian District, 100083, PR China.
E-mail: zhangmingxiang@bjfu.edu.cn

the pore scale arises from different controlling factors: soil texture and structure (Shein, 2010); soil bulk density (Reading *et al.,* 2012); soil water content (Kramers *et al.,* 2009; Sanders *et al.,* 2012); soil water repellency (Benito Rueda *et al.,* 2016; Alanís *et al.,* 2016; Malvar *et al.,* 2016; Santos *et al.,* 2016); soil cracks (Zhang *et al.,* 2015b); the soil shrink-swell phenomenon (Shein, 2010); soil biota (Cerdà *et al.,* 2009); land use (Hanson *et al.,* 2004; Cerdà & Doerr, 2007; Haghighi *et al.,* 2010; Yüksek *et al.,* 2010; Zema *et al.,* 2012; Leh *et al.,* 2013; Liu *et al.,* 2014; Wildemeersch *et al.,* 2015); vegetation (Cerdà, 1996; Cerdà, 1998a; Zhao *et al.,* 2016); climate changes (Cerdà, 1998c; Cerdà, 1998b); fire (Cerdà, 1998d; Granged *et al.,* 2011; Bodí *et al.,* 2012; Bodí *et al.,* 2013; León *et al.,* 2013; Hewelke *et al.,* 2016); plant roots (Bargués Tobella *et al.,* 2014; Zhang *et al.,* 2015a); rock fragments (Jomaa *et al.,* 2012; Hlaváčiková *et al.,* 2015; Pereira *et al.,* 2015; Zhang *et al.,* 2016a); and biopores, voids, earthworms, fissures, and fauna (Jarvis *et al.,* 2012; Banaszuk *et al.,* 2013; Han *et al.,* 2015; Yagüe *et al.,* 2016).

The evaluation of plant root hydrological responses have been hampered by difficulties associated with the mechanisms of soil water flow and solute transportation, particularly preferential flow (Ola *et al.,* 2015). Channels formed by plant roots and root–soil interfaces affect soil hydrological responses, such as water uptake, nutrient acquisition, solute retention, and soil conservation, during plant root growth. Plant roots grow into soil pores to form continuous preferential root channels (Tracy *et al.,* 2011). The relation between plant roots and preferential flow was described by Ceccon *et al.* (2011); Bargués Tobella *et al.* (2014), and Zhang *et al.* (2015a). Both living and decayed plant roots provide preferential flow paths for water flow and solute transportation (Backnäs *et al.,* 2012; Zhang *et al.,* 2015a; Zhang *et al.,* 2016b). Plant roots and the surrounding rhizosphere significantly influence land degradation by changing the preferential flow paths. It is well known that plant roots play a positive role in soil properties with high soil macroporosity, soil fertility, soil biodiversity, soil organisms, soil activity, low soil temperature, and soil evaporation (Cerdà, 1996; Bochet, 2015; Singh *et al.,* 2015). As such, plant roots affect the soil properties by increasing the soil aggregate stability and reinforcing the surrounding soil matrix (Vannoppen *et al.,* 2015). Plant roots with diverse architectures tend to be vitally important to shaping the soil environment and development from the soil surface to the subsurface (Brevik *et al.,* 2015; Ola *et al.,* 2015; Roy & McDonald, 2015). The rhizosphere, with abundant microorganisms and nutrients, is regarded as an ensemble that includes plant roots, microorganisms, rhizosheath, and soil surrounding plant roots and beneficially protects the soil against degradation by supporting soil aggregation (Ghestem *et al.,* 2011; Ni *et al.,* 2015; Ola *et al.,* 2015). Moreover, some relatively stable channels defined as preferential flow paths improve the chemical and biological activities in the rhizosphere together with the physical action of plant roots (Ghestem *et al.,* 2011). Plant roots are of vital importance in reducing soil erosion. The erosion–reducing potential of plant roots is correlated with the complex plant root–soil interaction, for instance, by changing soil hydrological properties and processes (e.g. soil water flow) (Vannoppen *et al.,* 2015). Jørgensen *et al.* (2002) stated that soil water flow and solute transportation were more evident in soil profiles with plant root channels than in profiles without plant root channels. Xin *et al.* (2016) found that water flow increased remarkably for soils with distributed macropores compared with soils without macropores. When a large variability in the soil water flow is observed, it is important to consider preferential flow properties because of the interaction between plant roots and soils (Vannoppen *et al.,* 2015). Many studies have investigated preferential flow in agricultural soils such as those of Willsboro, New York (Steenhuis *et al.,* 1988) and northwestern Mississippi in the USA (Perkins *et al.,* 2011); grassland soils in Ireland (Kramers *et al.,* 2009) and the Meijendel dune area north of the Hague, the Netherlands (Harkel *et al.,* 1998), whereas studies in stony soils located in rocky mountainous forest ecosystems are less frequent (Ni *et al.,* 2015). Rock fragments, stones, and plant roots within soil profiles constitute a complicated macropores network, which exerts significant influences on soil water flow. What is the interaction between plant roots and soil water flow in response to preferential flow paths in rocky mountainous forest ecosystems? How to identify the relation between plant root distribution and soil water flow in stony soils? These issues should be given more attention.

The present study was conducted to investigate the effects of preferential flow on plant roots and soil water flow in stony soils. The results have considerable relevance to studies of land degradation originating from preferential flow in addition to topsoil erosion and overland flow. In previous studies, soil water flow assessments were unclear with respect to preferential flow properties. The objectives of our study were (1) to evaluate fine plant root distribution in response to preferential flow paths; (2) to characterize the soil water flow of preferential flow paths; and (3) to quantitatively identify the relation between plant root distribution and soil water flow.

MATERIALS AND METHODS

Study Site

A field study was carried out at Jiufeng National Forest Park (116°28′E and 39°34′N) in Beijing, China (Figure 1). Jiufeng National Forest Park is part of Beijing Forestry University for teaching and scientific research and covers an area of approximately 832 ha. The park has an altitude ranging from 60 to 1,100 m above mean sea level (masl). The main climatic characteristics of the park are an average annual temperature of 11·6 °C and a mean maximum and minimum annual temperature of 41·6 °C and −19·6 °C, respectively. The climate is temperate continental with a mean annual precipitation of 630 mm and a mean annual potential evapotranspiration of 1,900 mm. A wide range of

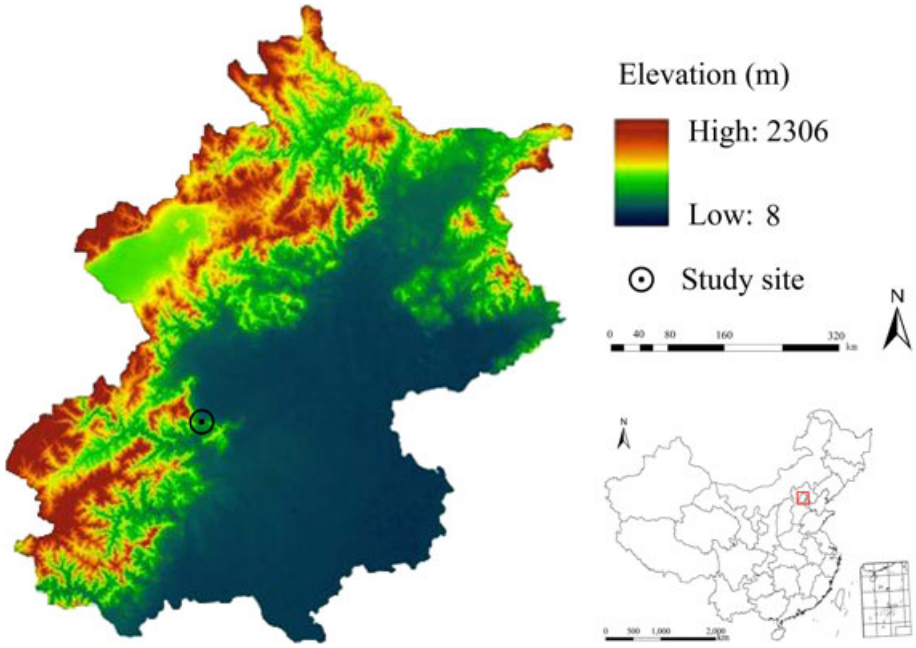

Figure 1. Sampling locations and geological map of the study site (source from *Geographical Information Monitoring Cloud Platform of China*) and location of Jiufeng National Forest Park. This figure is available in color online at wileyonlinelibrary.com/journal/ldr.

secondary forest types were observed below 800 masl, where the dominant vegetation were *Platycladus orientalis* (L.) *Franco*, *Pinus tabulaeformis* Carr., Oak (*Quercus* spp.), *Robinia pseudoacacia* L., and the shrubs *Prunus armeniaca* L. and *Vitex chinensis* (Mill.). Above 800 masl, *P. tabulaeformis* Carr., *Lespedeza bicolor*, *Spiraea trilobata*, and *Caragana rosea* dominated the sparse forest cover. According to the soil profiles in the field, the soils were rich in rock fragments. The soils in the study site were identified as Luvisols, and the soil texture was sandy loam, with an organic carbon content of between 2·28 and 46·17 g kg^{-1}. The soil pH ranged from 5·87 to 7·12 (Table I). The park is chosen as the case study site for the present research because the site greatly influences the groundwater security of northern China, particularly Beijing. Since 1960, several protective actions have been undertaken throughout the area.

Field Dye-tracing Experiments

Six experimental plots were established within a 10 × 10-m quadrat with similar site conditions, low-lying flat areas, and representative plant species at 260 masl. Plots 1 and 2 were located in the *S. japonica* Linn., plots 3 and 4 were in the *P. orientalis* (L.) *Franco*, and plots 5 and 6 were in the *Q. dentata* Thunb. sections of the quadrat. Preferential flow paths were identified by monitoring the movement of the colored solution added to each plot. The process of root growth/water flow was on the plant scale, and experimental plots were independent of each other. A Brilliant Blue FCF (C.I. Food Blue 2) dye solution (5 g L^{-1}) was applied to the experimental plots during the growth season. The solution was uniformly applied to a 1·2 × 1·2-m area centered on the experimental plants to avoid border effects. A total solution volume of 50 L was applied to each experimental plot. Vertical soil profiles with a maximum dye depth of 1·0 m were excavated from the center of the experimental plots 1 day after the dye tracer was applied and the solution had infiltrated the soil (Hu *et al.,* 2013). Two replicate horizontal soil cores were excavated from preferential flow paths and the surrounding soil matrix throughout the soil profile. Preferential flow paths were identified by the stained areas, and the surrounding soil matrix was identified by the unstained areas (Hanson *et al.,* 2004; Zhang *et al.,* 2015a).

Laboratory Analyses

Outside the canopy and 50 cm from the experimental plots, 36 undisturbed soil columns (7-cm diameter, 10 cm high) were extracted from the soil surface to a depth of 60 cm. Outside each experimental plot, six undisturbed soil columns were collected, and two soil columns were obtained from depths of 0–20, 20–40, and 40–60 cm, respectively. Studies of water flow in soil columns were conducted under different conditions maintaining (1) a constant hydraulic head of 1·0 cm of water with various solution concentrations of 0·5, 1·0, and 1·5 g L^{-1} and (2) a constant solution concentration of 1·0 g L^{-1} with various hydraulic heads of 0·5, 1·0, and 1·5 cm of water. Some soil columns were left to become saturated with water for at least 24 h, while others were unsaturated. After the wetting front reached the base of the soil columns, the effluent was continuously collected into plastic flasks over timed intervals every 1, 3, 5, and 10 min. The accumulated effluent samples were then measured with an ultraviolet spectrometer subsystem to determine the relative concentration (*RC*) of the accumulated effluent (Figure 2).

Table I. Soil physicochemical properties in the soil layers of different experimental plots

Experimental plots	SD (cm)	PSD			ST	RFC (%)	SOC (g kg^{-1})	pH
		Sand (%)	Silt (%)	Clay (%)				
Plot 1	0–15	55·5	26·8	17·7	Loamy soil	13·9	38·65	7·12
	15–30	63·7	19·9	16·4	Loamy soil	18·3	11·32	6·05
	30–50	67·7	19·7	12·6	Loamy soil	19·5	4·72	6·01
	50–60	65·5	22·9	11·6	Loamy soil	19·2	2·28	6·31
Plot 2	0–15	56·2	25·4	18·4	Loamy soil	11·2	36·82	6·89
	15–30	62·8	20·2	17·0	Loamy soil	16·8	13·12	6·10
	30–50	68·9	21·3	9·8	Loamy soil	19·4	3·98	5·98
	50–60	63·5	23·7	12·8	Loamy soil	18·9	2·37	6·04
Plot 3	0–15	59·4	23·1	17·5	Loamy soil	12·1	44·58	5·97
	15–30	65·2	18·2	16·6	Loamy soil	15·6	15·17	6·10
	30–50	66·4	18·4	15·2	Loamy soil	18·8	6·87	5·87
	50–60	63·8	19·7	16·5	Loamy soil	19·4	3·45	6·03
Plot 4	0–15	58·7	24·1	17·2	Loamy soil	12·8	46·17	6·00
	15–30	64·8	20·8	14·4	Loamy soil	16·7	17·20	6·05
	30–50	67·3	21·5	11·2	Loamy soil	19·5	5·89	5·97
	50–60	63·4	22·9	13·7	Loamy soil	18·4	3·64	6·04
Plot 5	0–15	57·3	23·5	19·2	Loamy soil	13·5	44·70	6·10
	15–30	64·8	24·4	10·8	Loamy soil	16·4	16·80	6·08
	30–50	65·7	21·5	12·8	Loamy soil	19·8	4·58	5·98
	50–60	63·4	22·4	14·2	Loamy soil	18·7	3·97	5·96
Plot 6	0–15	56·9	24·9	18·2	Loamy soil	11·8	42·80	6·00
	15–30	63·8	21·8	14·4	Loamy soil	16·8	15·21	6·04
	30–50	66·3	23·5	10·2	Loamy soil	18·9	4·87	6·21
	50–60	62·7	21·6	15·7	Loamy soil	18·4	2·89	6·11

SD, soil depth; PSD, particle size distribution; ST, soil texture; RFC, rock fragments content; SOC, soil organic carbon.

To obtain the *RC*, undisturbed soil columns of the soil layers (0–20, 20–40, and 40–60 cm) were measured under saturated and unsaturated soil conditions. The *RC* was calculated by

$$RC = C/C_0 \quad (1)$$

where C is the accumulated effluent concentration (g L^{-1}) and C_0 is the initial concentration of the solution (g L^{-1}).

The plant root–water interaction (*PRWI*) was defined as an indicator of the effects of plant root parameters (root length density) on the soil water flow process (changes in the soil water content) and was calculated by

$$\Phi = RLD_{PFP}(\theta_{PFP} - \theta) \text{ or } \Phi = RLD_{SM}(\theta_{SM} - \theta) \quad (2)$$

where Φ is the *PRWI*, RLD_{PFP} is the root length density in preferential flow paths (mm (100 cm^3)$^{-1}$), RLD_{SM} is the root length density in the surrounding soil matrix (mm (100 cm^3)$^{-1}$), θ_{PFP} is the soil water content in the preferential flow paths after the field dye-tracing experiments (cm^3 cm^{-3}), θ_{SM} is the soil water content in the surrounding soil matrix after the field dye-tracing experiments

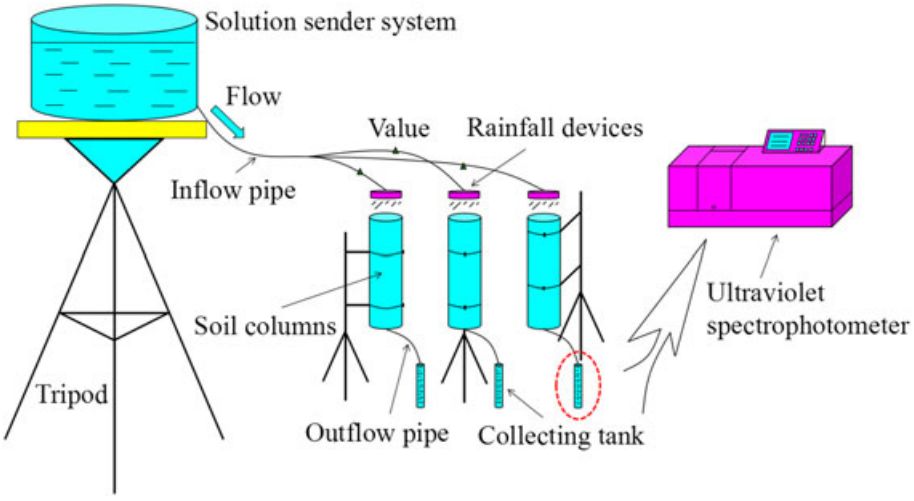

Figure 2. Experimental setup of soil water flow and solute transportation. This figure is available in color online at wileyonlinelibrary.com/journal/ldr.

($cm^3\,cm^{-3}$), and θ is the initial soil water content of the experimental site ($cm^3\,cm^{-3}$).

Fine Plant Root Sampling

Plant species including *S. japonica* Linn., *P. orientalis* (L.) *Franco*, and *Q. dentata* Thunb. were characterized at the study site. To determine the spatial distribution of the fine plant roots in the soil profiles, soil samples were taken at each soil depth using soil cores (5-cm diameter, 5 cm high) with two replicates from the preferential flow paths and the surrounding soil matrix. Horizontal soil cores from the soil profile were excavated in 10-cm intervals 24 h after the application of the Brilliant Blue FCF dye solution, and soil samples were taken from depths of 0 to 10, 10 to 20, 20 to 30, 30 to 40, 40 to 50, and 50 to 60 cm depending on the maximum dye infiltration depth. At least nine soil profiles were extracted starting from each plot boundary to the center of the target plant. In total, we collected 100 soil cores. Soil samples were then removed from the soil cores, placed in plastic bags, numbered, and stored under refrigeration (4 °C) prior to the separation of the fine plant roots.

Measurement of Fine Plant Root Parameters

When necessary, soil samples were initially soaked in water for several hours, and then, the soil was separated from the roots under running water using 5-mm mesh sieves. Soil samples were placed in dishes with 4–5 mm of water so that the plant roots could spread and the soil particles could be easily removed (Yan *et al.,* 2011). The roots from the soil samples were gently washed to remove the soil particles and debris. The fine plant roots were then sorted into their respective plant species. The fine roots of the separate plant species were then dried for 48 h in an oven at 70 °C and scanned and analyzed using the WinRHIZO (STD4800) root analysis system (Yan *et al.,* 2011) for morphological parameter measurements, such as root length density (mm $(100\,cm^3)^{-1}$). Root length density (total root length per soil volume) (Glab, 2013) is typically measured using a measuring tape (Singh *et al.,* 2015). We defined fine root diameter as ≤5 mm, which has been commonly used in other studies (Finér *et al.,* 2011).

Data Analysis

Results of the soil water flow process from the two treatments (constant hydraulic head of 1 cm of water and constant solution concentration of $1\,g\,L^{-1}$) were determined by statistically analyzing the data. One-way analysis of variance and the least significance difference (LSD) *post hoc* test were used to compare the differences in the initial time, initial relative concentration, and final relative concentration of the accumulated effluent under saturated and unsaturated soil conditions and the differences in root length density for preferential flow paths within the three plant species and among the soil depths. The Pearson correlation coefficient was used to evaluate the relation between plant root distribution and soil water flow. The results were reported at a 5% level of significance. Regression analysis was conducted to indicate the effects of plant root distribution on soil water flow. The coefficient of determination (R^2) was used to evaluate the performance of the applied regression equations. Data were analyzed using Statistical Package for the Social Sciences statistical analysis software.

RESULTS

Soil Water Flow Process and the Relative Concentration of the Accumulated Effluent

Soil columns under saturated conditions

Results of the soil water flow process and the relative concentration of the accumulated effluent with different treatments (constant hydraulic head of 1 cm of water and constant solution concentration of $1\,g\,L^{-1}$) under saturated soil conditions are shown (Figure 3). The initial accumulated effluent time significantly varied at different soil depths (0–20, 20–40, and 40–60 cm) with a constant solution concentration of $1{\cdot}0\,g\,L^{-1}$ (R^2-adj = 0·869, $p < 0{\cdot}05$), whereas there were no significant ($p > 0{\cdot}05$) differences among the three hydraulic heads of water (0·5, 1·0, and 1·5 cm) (Figure 3a, b, and c). A higher significant ($p < 0{\cdot}05$) difference in the initial accumulated effluent time with a constant solution concentration of $1{\cdot}0\,g\,L^{-1}$ was found in the 0–20-cm soil columns than in the 40–60-cm soil columns. The initial accumulated effluent time in Figure 3a, b, and c ranged from 5–70 s in all of the treatment comparisons. There were no significant ($p > 0{\cdot}05$) differences in the initial relative concentration of the accumulated effluent among the three hydraulic heads of water (0·5, 1·0, and 1·5 cm) and among the three soil depths (0–20, 20–40, and 40–60 cm) under a constant solution concentration of $1{\cdot}0\,g\,L^{-1}$. However, significant (R^2-adj = 0·827, $p < 0{\cdot}05$) differences in the final relative concentration of the accumulated effluent with a constant solution concentration of $1{\cdot}0\,g\,L^{-1}$ were found among the three soil depths, and a higher significant ($p < 0{\cdot}05$) difference was found in the 0–20-cm soil columns than in the 40–60-cm soil columns.

There were no significant ($p > 0{\cdot}05$) differences in the initial accumulated effluent time among the three solution concentrations (0·5, 1·0, and $1{\cdot}5\,g\,L^{-1}$) with a constant hydraulic head of 1 cm of water (Figure 3d, e, and f). The initial accumulated effluent time was significantly lower in the 0–20-cm soil columns than in the 20–40 and 40–60-cm soil columns. The initial accumulated effluent time increased with soil depth (R^2-adj = 0·687, $p < 0{\cdot}05$). Significant ($p < 0{\cdot}05$) differences in the initial accumulated effluent time were observed among the three soil depths (0–20, 20–40, and 40–60 cm) (Figure 3d, e, and f). For soil depth, a higher significant ($p < 0{\cdot}05$) difference in the initial accumulated effluent time was found in the 0–20-cm soil columns than in the 40–60-cm soil columns. The initial accumulated effluent time in Figure 3d, e, and f ranged from 14–62 s in all of the treatment comparisons. Furthermore, there were no significant ($p > 0{\cdot}05$) differences in the initial relative concentration of the accumulated effluent among the three solution concentrations (0·5, 1·0, and $1{\cdot}5\,g\,L^{-1}$) and among

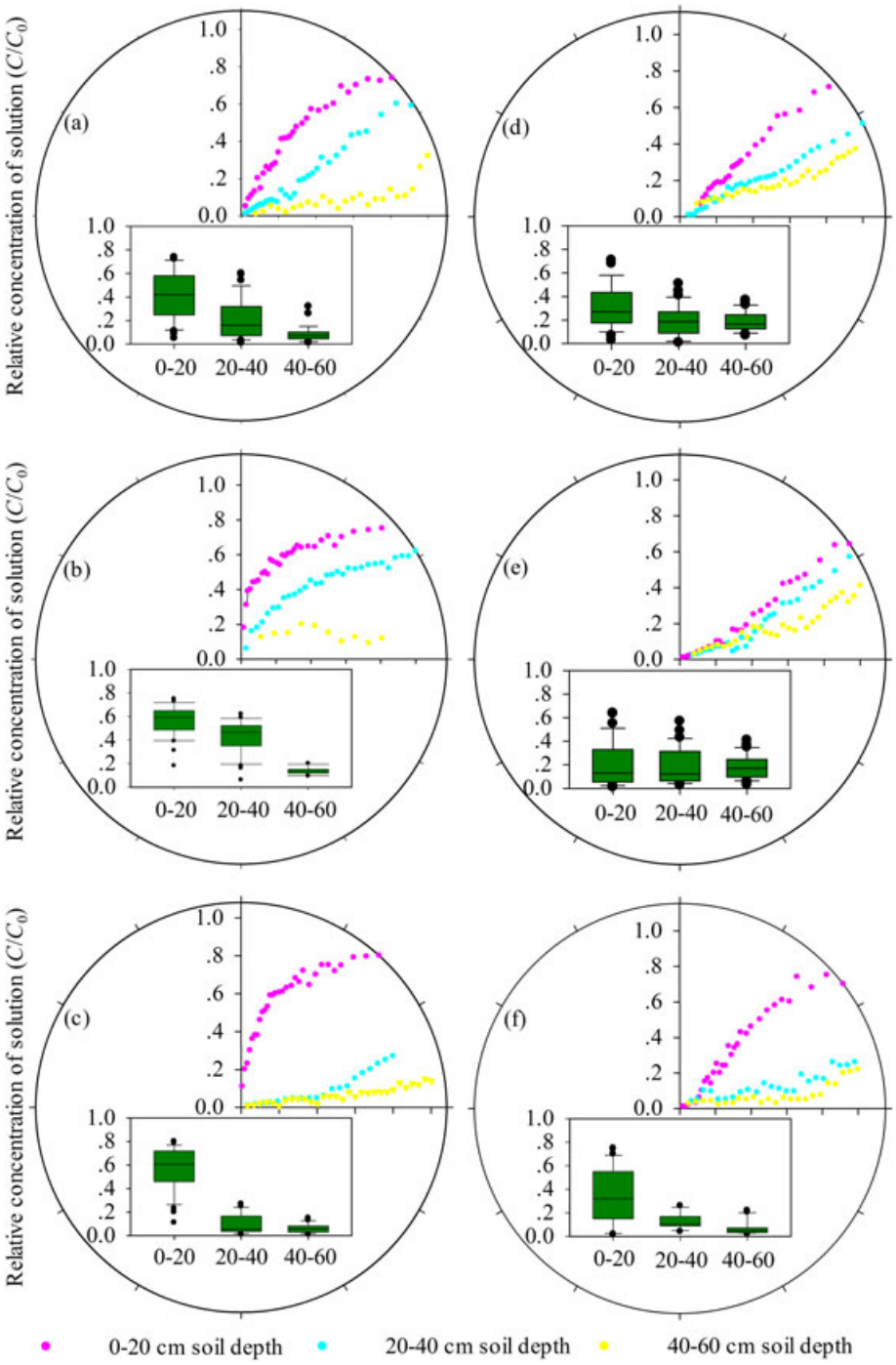

Figure 3. Changes in the relative concentration of the accumulated effluent with time and soil depth under saturated soil conditions. (a), (b), and (c) were conducted with a constant solution concentration of 1·0 g L^{-1} with different hydraulic heads of 0·5, 1·0, and 1·5 cm of water, respectively; (d), (e), and (f) were conducted with a constant hydraulic head of 1·0 cm of water with different solution concentrations of 0·5, 1·0, and 1·5 g L^{-1}, respectively. The initial and final relative concentrations of the accumulated effluent are illustrated for soil depths of 0–20, 20–40, and 40–60 cm. The results of the initial time (R^2-adj = 0·869, $p < 0·05$) and the initial ($p > 0·05$) and final (R^2-adj = 0·827, $p < 0·05$) relative concentration of the accumulated effluent among the three soil depths for (a), (b), and (c); and the initial time (R^2-adj = 0·687, $p < 0·05$) and the initial ($p > 0·05$) and final (R^2-adj = 0·713, $p < 0·05$) relative concentration of the accumulated effluent for (d), (e), and (f), respectively, are presented at a 5% level of significance according to the least significance difference *post hoc* test. This figure is available in color online at wileyonlinelibrary.com/journal/ldr.

the three soil depths (0–20, 20–40, and 40–60 cm) under a constant hydraulic head of 1 cm of water. However, significant (R^2-adj = 0·713, $p < 0·05$) differences in the final relative concentration of the accumulated effluent were found among the three soil depths, and a higher significant ($p < 0·05$) difference was found in the 0–20-cm soil columns than in the 40–60-cm soil columns. The relative concentration of the accumulated effluent increased with time and decreased with soil depth under saturated soil conditions. The curve of the 0–20-cm soil columns increased relatively quickly and remained above at the other two soil depths during the entire process (Figure 3).

Soil columns under unsaturated conditions

Results of the soil water flow process and the relative concentration of the accumulated effluent with different treatments (constant hydraulic head of 1 cm of water and constant solution concentration of $1\,g\,L^{-1}$) under unsaturated soil conditions are shown (Figure 4). There were no significant ($p > 0{\cdot}05$) differences in the initial accumulated effluent time, the initial relative concentration

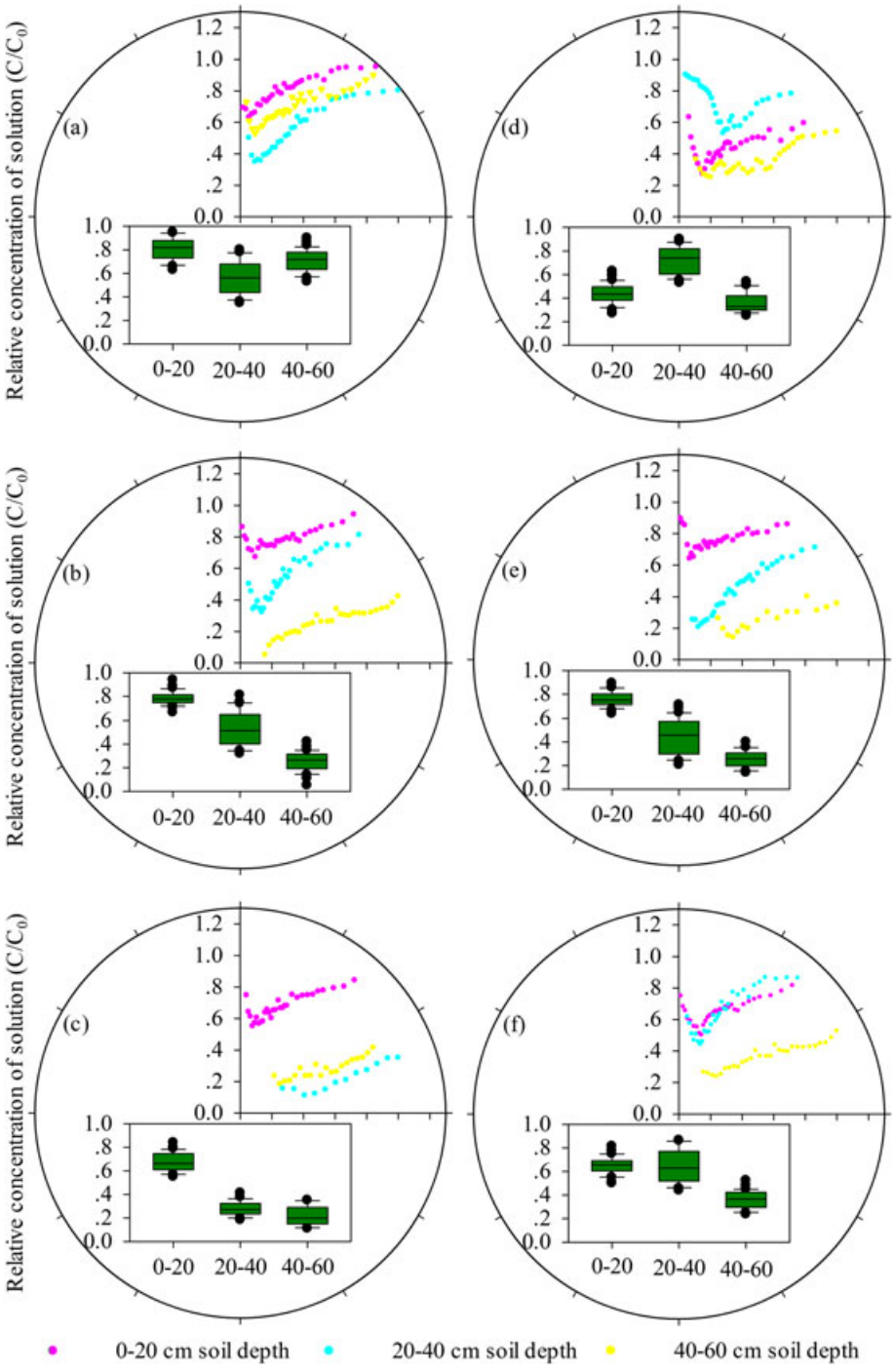

Figure 4. Changes in the relative concentration of the accumulated effluent with time and soil depth under unsaturated soil conditions. (a), (b), and (c) were conducted with a constant solution concentration of $1{\cdot}0\,g\,L^{-1}$ with different hydraulic heads of 0·5, 1·0, and 1·5 cm of water, respectively; (d), (e), and (f) were conducted with a constant hydraulic head of 1·0 cm of water with different solution concentrations of 0·5, 1·0, and $1{\cdot}5\,g\,L^{-1}$, respectively. The initial and final relative concentrations of the accumulated effluent are illustrated for soil depths of 0–20, 20–40, and 40–60 cm, respectively. The results of the initial time ($p > 0{\cdot}05$) and the initial ($p > 0{\cdot}05$) and final ($p > 0{\cdot}05$) relative concentrations of the accumulated effluent among the three soil depths for (a), (b), and (c); and the initial time (R^2-adj = 0·654, $p < 0{\cdot}05$) and the initial ($p > 0{\cdot}05$) and final (R^2-adj = 0·713, $p < 0{\cdot}05$) relative concentration of the accumulated effluent for (d), (e), and (f), respectively, are presented at a 5% level of significance according to the least significance difference *post hoc* test. This figure is available in color online at wileyonlinelibrary.com/journal/ldr.

of the accumulated effluent, and the final relative concentration of the accumulated effluent among the three hydraulic heads of water (0·5, 1·0, and 1·5 cm) and among the three soil depths (0–20, 20–40, and 40–60 cm) under a constant solution concentration of $1{\cdot}0\,g\,L^{-1}$. The initial accumulated effluent time in Figure 4a, b, and c ranged from 36–1,940 s in all of the treatment comparisons.

The initial accumulated effluent time under a constant hydraulic head of 1 cm of water was lower in the 0–20-cm soil columns than in the 20–40 and 40–60-cm soil columns (Figure 4d, e, and f). The initial accumulated effluent time increased with soil depth (R^2-adj = 0·654, $p < 0{\cdot}05$). For soil depth, a higher significant ($p < 0{\cdot}05$) difference for the initial accumulated effluent time under a constant hydraulic head of 1 cm of water was found in the 0–20-cm soil columns than in the 40–60-cm soil columns. No significant ($p > 0{\cdot}05$) differences in the initial accumulated effluent time among the three solution concentrations (0·5, 1·0, and $1{\cdot}5\,g\,L^{-1}$) were found. The initial accumulated effluent time in Figure 4d, e, and f ranged from 37–2,130 s in all of the treatment comparisons. With respect to the initial relative concentration of the accumulated effluent, no significant ($p > 0{\cdot}05$) differences among the three solution concentrations (0·5, 1·0, and $1{\cdot}5\,g\,L^{-1}$) or among the three soil depths (0–20, 20–40, and 40–60 cm) under a constant hydraulic head of 1 cm of water were found. For the final relative concentration of the accumulated effluent, significant (R^2-adj = 0·713, $p < 0{\cdot}05$) differences were found among the three soil depths, and a higher significant ($p < 0{\cdot}05$) difference was found in the 0–20-cm soil columns than in the 40–60-cm soil columns. The relative concentration of the accumulated effluent under unsaturated soil conditions initially decreased and then increased with time (Figure 4).

Fine plant root distribution for preferential flow paths

The results showed that the change in the root length density (RLD) with soil depth was similar. The RLD, which had a root diameter class (≤5 mm) for preferential flow paths in all of the experimental plots and contained three types of plants, decreased with soil depth (Table II). The largest RLD was recorded in the upper soil layers to a depth of 20 cm, and approximately half the RLD was measured from the soil surface to this soil layer. This result also reflected the fact that the lowest RLD was recorded in the subsoil. The RLD of the preferential flow paths made up at least 50% of the total RLD at each soil depth (Table II). Fine plant root distribution of preferential flow paths as evaluated by the maximum dye infiltration depth varied among the different experimental plots, and the average maximum dye infiltration depth was higher in experimental plots 1, 3, and 5 than in plots 2, 4, and 6 (Table II). The variations in the RLD from the preferential flow paths among the three plant species showed statistically significant differences ($p < 0{\cdot}05$). The RLD from the preferential flow paths varied among the soil depths (R^2-adj = 0·510, $p < 0{\cdot}05$).

Relation between fine plant root distribution and soil water flow

The effects of plant root distribution on changes in the soil water content are shown (Figure 5 and Table III). Overall, the *PRWI* increased with increasing root length density with a high correlation coefficient (R^2-adj = 0·502, $p < 0{\cdot}05$, $N = 50$). Thus, all samples with a *PRWI* above 0 were from the areas where the soil water content increased after the field dye-tracing experiments compared with the initial soil water content, while samples with a *PRWI* less than 0 were from the areas where the soil water content decreased after the field dye-tracing experiments compared with the initial soil water content. As shown in Figure 4 and Table III, there were 33 samples with a *PRWI* above 0 and 17 samples with a *PRWI* less than 0. The proportion of samples with a *PRWI* above 0 was approximately 66%, and the proportion of samples with a *PRWI* less than 0 was approximately 34%.

DISCUSSION

Soil Water Flow with Preferential Flow Paths in Laboratory Analyses

A lower initial accumulated effluent time can be related to higher soil organic matter causing lower soil bulk density and higher total soil porosity at a soil depth of 0–20 cm (Haghighi *et al.,* 2010; De Boever *et al.,* 2014). Lower soil bulk density is also caused by abundant plant roots, which enhance the preferential flow paths and promote soil water flow and solute transportation from the surface (Singh *et al.,* 2015). Therefore, soil development and soil activities enhanced by improved soil properties are vitally important in the soil hydrological process (e.g. soil water flow) and soil water infiltration rates (Cerdà, 1998a; Haghighi *et al.,* 2010; Wang *et al.,* 2016).

Overall, we found that the relative concentration of the accumulated effluent under saturated soil conditions increased with time and decreased with soil depth. This result was consistent with that reported by Zhou *et al.* (2010, 2011). The soil pore space in soil columns was full of water under saturated conditions. Water may concentrate in macropores and cause preferential flow paths, leaving the surrounding soil matrix relatively dry (Malvar *et al.,* 2016). Preferential flow paths and the large macropores carried most of the water when the soils became saturated (Hanson *et al.,* 2004). As the solution was applied to the surface of the soil columns, water might have flowed along the soil pores because of external water pressure. A solution with a low concentration was collected at the beginning of the accumulated effluent. Our results also indicated that the relative concentration of the accumulated effluent under unsaturated soil conditions initially decreased and then increased with time. The initial relative concentration of the accumulated effluent was high because the solution tended to transport through the soil columns via preferential flow paths without resistance. This phenomenon was attributed to preferential flow. Solutions with higher concentrations and faster infiltration were common in the 0–20-cm soil depth compared with

Table II. Statistics of root length density in preferential flow paths and the surrounding soil matrix with soil depth and the maximum dye infiltration depth into soil profiles in different experimental plots

Plant species	Experimental plots	Soil depth (cm)	RLD		Proportion (%)[a]	Proportion (%)[b]	MDID					
			RLD_{PFP}	RLD_{SM}			Maximum	Minimum	Mean	Variation	SD	CV
Sophora japonica Linn.	Plot 1	0–10	2,284	1,690	57	55	50	34·5	42·1	29·39	5·42	0·13
		10–20	1,844	1,595	54							
		20–30	1,315	1,167	53							
		30–40	1,032	859	55							
		40–50	735	581	56							
	Plot 2	0–10	2,248	2,084	52	54	49	35·9	41·4	21·43	4·63	0·11
		10–20	1,807	1,820	50							
		20–30	1,099	897	55							
		30–40	960	675	59							
Platycladus orientalis (L.) *Franco*	Plot 3	0–10	3,720	1,560	70	63	69·5	35	50·6	132·22	11·5	0·23
		10–20	2,363	1,283	65							
		20–30	877	799	52							
		30–40	717	393	65							
		40–50	683	269	72							
		50–60	174	151	54							
	Plot 4	0–10	4,456	2,254	66	63	32·2	17·5	24·7	21·74	4·66	0·19
		10–20	3,237	1,961	62							
		20–30	2,889	1,310	69							
		30–40	1,593	1,428	53							
Quercus dentata Thunb.	Plot 5	0–10	3,221	1,735	65	61	50·2	39·1	43·2	9·58	3·09	0·07
		10–20	1,939	1,050	65							
		20–30	1,292	1,199	52							
	Plot 6	0–10	3,310	2,200	60	56	42·2	22·4	29·3	55·12	7·42	0·25
		10–20	2,612	1,803	59							
		20–30	1,831	1,954	48							

RLD, root length density; RLD_{PFP}, root length density in preferential flow paths; RLD_{SM}, root length density in the surrounding soil matrix; MDID, the maximum dye infiltration depth; SD, standard deviation; CV, coefficient of variation.

[a]Represented the proportion of root length density in preferential flow paths to the total root length density each soil depth.

[b]Represented the proportion of root length density in preferential flow paths to the total root length density in the soil profiles.

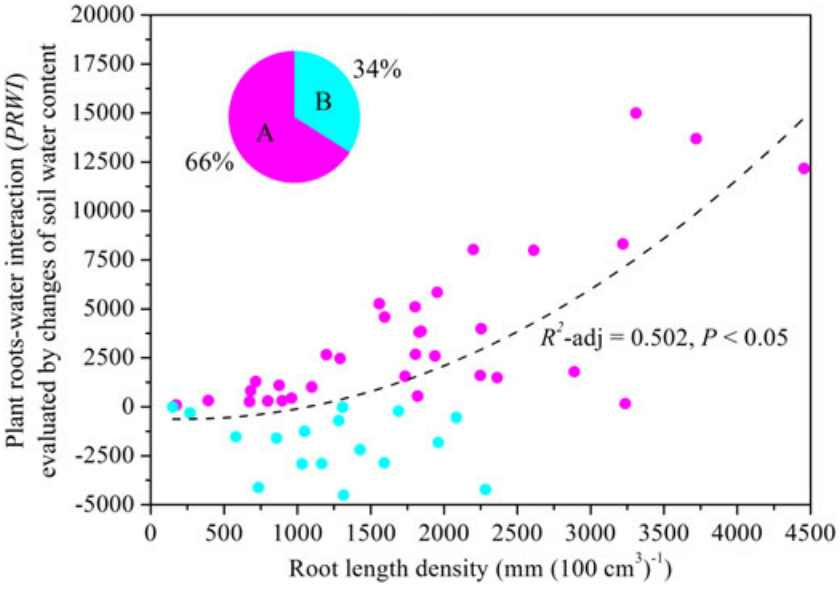

Figure 5. Relation between root length density and the plant root–water interaction (*PRWI*) in all of the experimental plots. All samples with a *PRWI* above 0 were from the areas where the soil water content increased after the field dye-tracing experiments compared with the initial soil water content, while samples with a *PRWI* less than 0 were from the areas where the soil water content decreased after the field dye-tracing experiments compared with the initial soil water content. A (the red circles) represented the proportion of samples with a *PRWI* above 0 was approximately 66%, and B (the blue circles) represented the proportion of samples with a *PRWI* less than 0 was approximately 34%. $N = 50$ for the *PRWI* in all experimental plots. This figure is available in color online at wileyonlinelibrary.com/journal/ldr.

the other depths (20–40 and 40–60 cm). The 0–20-cm soil depth was regarded as topsoil with higher soil macroporosity, soil organic matter, soil microorganisms, and soil activity and lower soil bulk density, soil evaporation, and soil temperature. Soil macroporosity, as an indicator of a dense soil pore network (Katuwal *et al.,* 2015b), is an essential factor contributing to soil structure. The heterogeneity of soil pore space affects the preferential water flow, heat, and solutes (Shein, 2010). The rapid transportation of substances through soil pore space is characterized by the high input rates of water (exceeding the rates of water absorption) to the upper soil surface (Shein, 2010). Soil pore size distribution also might be an important controlling factor (Haghighi *et al.,* 2010), and soil pore size of at least 10 µm in diameter could promote more liquid movement. Not all macropores contribute to water flow and solute transportation because of macropore connectivity and tortuosity. Studies have shown that 30% of macropore networks could form macropore flow and preferential flow paths to accelerate water flow and solute transportation (Sammartino *et al.,* 2012). However, there is still no clear understanding of the effects of soil pore architecture (e.g. soil pore size, geometry, connectivity, volume, surface area, and percentage) on preferential flow (Shein, 2010; Blunt *et al.,* 2013). A distinct early turning point in the soil water flow process was observed in the 0–20-cm soil depth with a higher macroporosity (Figure 4). The earlier turning point in the soil water flow process implied less dye tracer exchange between the preferential flow paths and the surrounding soil matrix. The results were in agreement with those reported by Katuwal *et al.* (2015b). However, the relative concentration of the accumulated effluent in our study was occasionally

Table III. Changes in the soil water content with soil depth in all of the experimental plots

Experimental plots	Soil depth (cm)	SWC[a]	SWC[b]	SWC[c]
Plot 1	0–10	19·19	17·34	19·06
	10–20	15·43	17·52	18·30
	20–30	15·72	12·29	13·23
	30–40	14·59	11·76	12·72
	40–50	15·97	10·36	13·33
Plot 2	0–10	12·90	13·61	12·64
	10–20	11·61	13·09	11·91
	20–30	11·71	12·63	12·05
	30–40	12·27	12·73	12·66
Plot 3	0–10	14·53	18·21	17·90
	10–20	14·28	14·91	13·73
	20–30	12·93	14·18	13·30
	30–40	12·54	14·34	13·35
	40–50	13·48	14·67	12·30
	50–60	14·29	14·83	14·20
Plot 4	0–10	9·91	12·64	11·68
	10–20	12·46	12·51	11·53
	20–30	11·29	11·91	11·27
	30–40	12·60	10·80	11·06
Plot 5	0–10	15·33	17·91	16·23
	10–20	13·44	14·78	12·24
	20–30	11·79	13·70	14·01
Plot 6	0–10	12·22	16·75	15·87
	10–20	9·70	12·76	12·53
	20–30	9·01	11·09	12·00

SWC, soil water content.
[a]Represented the initial SWC.
[b]Represented SWC in preferential flow paths after field dye-tracing experiments.
[c]Represented SWC in the surrounding soil matrix after field dye-tracing experiments, respectively.

higher at the 20–40-cm soil depth than at the 0–20-cm soil depth or higher at the 40–60-cm soil depth than at the 20–40 cm soil depth. These results might be more related to soil spatial heterogeneity, specifically macropore connectivity and tortuosity (Larsbo *et al.,* 2014a; Larsbo *et al.,* 2014b; Katuwal *et al.,* 2015a; Naveed *et al.,* 2015). Although some studies stated that the effects of soil compaction on preferential flow might be partly attributed to a reduction in the volume and connectivity of macropores (Mossadeghi-Björklund *et al.,* 2016), moderate soil compaction could increase the strength of preferential flow with few continuous macropores remaining. With respect to soil columns at the 40–60-cm soil depth, this soil layer exhibited a higher soil bulk density compared with the 20–40-cm soil depth. We could consider the soil bulk density at the 40–60-cm soil depth to be moderate soil compaction (Nosalewicz & Lipiec, 2014).

At our study site of rocky mountainous areas, the rock–soil interface, defined as soil cracks, might be the controlling factor for soil pore architecture. Zhang *et al.* (2013) found that the soil water infiltration rate was higher in young paddy fields with soil cracks. Zhang *et al.* (2015b) concluded that the structure of soil cracks was complex and that many irregular branches of soil cracks led to water reaching greater depths. The present study site was located in northern China and had abundant rock fragments. Rock fragments constituted a large portion of the soil profiles in Jiufeng National Forest Park, and the rock fragments content increased from the soil surface. Our study indicated that the initial accumulated effluent time increased with soil depth. This result was in agreement with that reported by Zhou *et al.* (2010). Zhou *et al.* (2010, 2011) stated that the water infiltration rate increased when the rock fragments content was $>40\%$ and that no abundant rock–soil interface was established when the rock fragments content was $<40\%$. Their finding was similar to our results. However, the rock–soil interface in stony soils was usually determined to be preferential flow paths. Water infiltration and deep penetration occurred because of the interface between rock fragments and the surrounding soil matrix. The rock–soil interface favored faunal activity and macropore density, specifically more preferential flow paths (Cerdà, 2001).

In the present study, we found that preferential flow initially affected changes in the relative concentration of the accumulated effluent and soil water flow process under unsaturated soil conditions. Soil water flow and solute transportation through preferential flow paths occurred initially without resistance, and the degree of interaction between the solution and soil interface increased with time. The interaction balanced out as the effects of preferential flow weakened and the surrounding soil matrix flow dominated. The surrounding soil matrix should not be assumed to be constant; otherwise, accumulated effluent time and concentration would be underestimated when researchers use the dual-permeability numerical model (Coppola *et al.,* 2015). We also found that the relative concentration of the accumulated effluent increased and that the soil matrix flow was predominant. This result was similar to that of Zhou *et al.* (2010, 2011). The variation in the soil water flow process might be caused by the lateral infiltration of the soil profile. The lateral infiltration phenomenon was common for soil water flow and solute transportation. The flow patterns led to high fluctuations in water flow time, accumulated effluent concentration, preferential flow degree and properties. However, preferential flow paths could not be fully developed by water applied to the surface of soil columns without enough water pressure.

Soil Water Flow with Preferential Flow Paths in Field Dye-tracing Experiments

Our study indicated that the maximum depth of dye infiltration into soil profiles was different among the plant species and also within the same vegetation type. These results were consistent with those of Beven & Germann (1982) and Jarvis (2007), who found that a higher initial soil water content (SWC) increased the depth of macropore flow penetration in macroporous soils because of the decreased lateral flow into the surrounding soil matrix. In the present study, the initial SWC was higher in experimental plots 1, 3, and 5 than in plots 2, 4, and 6. This difference has been associated with more soil organic matter in wet soils than in dry soils (Nocita *et al.,* 2013); thus, a higher soil water content could be ascribed to high soil organic matter (Haghighi *et al.,* 2010). In wet soils, soil microorganism activities are reduced, resulting in the decreased decomposition of soil organic matter (Goebel *et al.,* 2011). For stony soils in forests, the specific soil texture type, vegetation cover, and soil physicochemical properties exerted different effects on the soil hydrological responses depending on the study site. However, some authors have been unable to consistently determine the hydrological response with the widespread assumption that water infiltration into the subsoil via preferential flow paths is markedly higher in wet soils than in dry soils. Hanson *et al.* (2004) found that deep percolation occurred during dry seasons. Merdun *et al.* (2008) reported that preferential flow was more evident when soil was initially dry. This finding may have been the result of using samples collected at a specific time of the year or because the authors included soils with different soil textures, organic carbon contents, and pH as well as different plant species (Benito Rueda *et al.,* 2016).

Our results revealed a significant influence on the maximum dye infiltration depth from the initial SWC; this may have been the result of the interaction between the SWC spatial patterns and soil water repellency (Jordán *et al.,* 2008). Soil water content is an essential component of soil water repellency dynamics (Benito Rueda *et al.,* 2016; Hewelke *et al.,* 2016). Soil water repellency is found to be eliminated during extremely wet weather and be most severe during dry periods because it can result in changes in the soil hydrological responses and the soil water content spatial patterns (Rodríguez-Alleres & Benito, 2011; Rodríguez-Alleres *et al.,* 2012). Our field dye-tracing experiments were conducted during the extremely wet season, and the wet

season could even eliminate soil water repellency (Benito Rueda *et al.,* 2016). The main soil hydrological response of the eliminating soil water repellency is a reduction in runoff generation promoting preferential flow and soil infiltration capacity during wet periods (Alanís *et al.,* 2016). The preferential flow phenomenon was more evident during the sample collection process. Preferential flow is an important factor in soil water repellency because it affects the changes in the soil water content (Brevik *et al.,* 2015). During extremely wet periods, soils with even eliminating soil water repellency probably promote rapid water percolation into the subsoil via preferential flow paths and reduce soil water flow into the surrounding soil matrix (Cerdà, 1996), which exerts significant influences on the loss of soil nutrients and soil fertility, resulting in extreme soil degradation (Brevik *et al.,* 2015). Understanding these results is critical to preventing landslides and protecting soils from degradation.

Overall, the SWC collected from soil profiles after field dye-tracing experiments was higher in preferential flow paths than in the surrounding soil matrix (Table III). This conclusion is similar to the results obtained by Jiang *et al.* (2015), who reported that SWC was higher when obtained from a spatial distribution in the selected soil profile with heavily stained concentrations. Shinohara & Otsuki (2015) concluded that the spatial variation of SWC was higher in a bamboo stand than in a broadleaved stand and that well-developed preferential flow paths in the soil profiles might predominate. The degree of soil water flow and potential water percolation processes in preferential flow paths was reflected better with the spatial distribution of SWC (Jiang *et al.,* 2015). Preferential flow properties exert significant influences on SWC.

Fine Plant Root Distribution

Our results implied that fine plant roots with preferential flow paths decreased with soil depth for all experimental plots (Table II). The results are in agreement with those reported by Bengough (2012); Tracy *et al.* (2013); DuPont *et al.* (2014), and Ferchaud *et al.* (2015). Plant roots with millions of lateral branches associated with mycorrhizal hyphae constitute a complex system (Wu *et al.,* 2014; Mardhiah *et al.,* 2016). The complex system is an important factor in soil water uptake, nutrient transfer, soil water conservation, and fertility absorption. During plant root growth, fine plant roots not only grow into preferential flow paths but also generate preferential flow paths (biopores, cracks, and burrows) (Noguchi *et al.,* 1997). Fine plant roots begin decaying or decayed at a higher rate because their growth cycle is shorter than that of coarse plant roots. Furthermore, the longevity of fine plant roots ranges from a few months to years depending on the fine plant root turnover process, in which new roots replace decaying or decayed roots. The process is related to soil nutrient availability (Yavitt *et al.,* 2011). The preferential flow paths left by these roots are regarded as preferential root channels. Preferential root channels along the root surface promote root growth during the fine plant root decomposition process. Studies have shown that as fine plant roots decomposed into more organic matter, more preferential root channels would form. Thus, decaying or decayed roots would more effectively generate preferential flow paths than living roots (Zhang *et al.,* 2015a). Fine plant roots can also release complex organic compounds (e.g. amino acids and organic acids) into the soil to promote plant growth (Bengough, 2012). Concentrations of organic compounds in preferential flow paths were found to be 10–70% higher than that in the surrounding soil matrix. Bogner *et al.* (2010) showed that RLD was greater in preferential flow paths than in the surrounding soil matrix.

In our study, the highest RLD was recorded in the upper soil layers to a depth of 20 cm. These results are in agreement with those reported by Bogner *et al.* (2010); Glab (2013); Raizada *et al.* (2013), and Ni *et al.* (2015). Fine plant roots in the upper soil layers generate more preferential flow paths during the decomposition process (Jørgensen *et al.,* 2002). Fine plant roots in the upper soil layers can improve the soil physicochemical properties (e.g. soil bulk density, porosity, organic carbon, citation exchange capacity, organisms, fertility, aggregation, and activity). For example, soil surface layers have a higher recharge rate than the subsoil (Cai & Ofterdinger, 2016; Duncan *et al.,* 2016). Short-lived and non-woody fine plant roots might generate more preferential root channels. These results are in agreement with those reported by Noguchi *et al.* (1997), who stated that decaying alfalfa fine plant roots could generate more stable preferential flow paths than wheat roots. Our study also showed that RLD collected from each soil layer differed within the same plant species (Table II). The soil physicochemical properties and site description were similar in addition to plant species age. Studies have reported that fine plant roots increase with age. These results were similar to our findings. For example, we found that the fine plant roots collected from *P. orientalis* (L.) *Franco* and *Q. dentata* Thunb. increased over time. However, there were no significant differences in the fine plant roots collected from *S. japonica* Linn., which supported the findings of Ruark & Bockheim (1987) and Finér *et al.* (1997).

Relation Between Plant Root Distribution and Soil Water Flow

Considering the importance of plant roots for soil water flow, the key question was how plant roots from different plots affect the spatial patterns of soil water flow. We found a positive correlation between fine plant roots and changes in the SWC for all experimental plots. These results are consistent with those of Krounbi & Lazarovitch (2011); Nosalewicz & Lipiec (2014), and Ferchaud *et al.* (2015). Plant roots affected the spatial distribution of water flow and percolation. Soil water flow along with root–soil interface (preferential root channels), where plant roots are best able to withstand drought, has been extensively characterized. Studies have indicated that changes in the SWC are substantially greater in areas near the base of the plants than far away from the plants.

In the present study, we also found that the plant root–water interaction occurred even at depths without many plant roots. There was still soil water flow transfer with high heterogeneity from preferential flow paths to the surroundings or from the soil matrix to the surroundings in the subsoil. It is possible that coarse plant roots were primarily located in the subsoil, and these coarse plant roots might generate larger air gaps between the plant roots and soil in case of a drought to enhance water penetration (Bodner *et al.,* 2014). Indeed, preferential flow paths were observed in this soil layer by Chen & Weil (2010) and Perkons *et al.* (2014). Moreover, plant roots in the subsoil enhanced the use of reliable water from the subsoil (Ni *et al.,* 2015). A higher soil bulk density in the subsoil was defined as moderate soil compaction, which also preserved the root–soil contact (Nosalewicz & Lipiec, 2014). Soil water flow, water uptake, and water transfer in the soil–plant–water system occurred heterogeneously. Preferential flow paths greatly affect their surroundings, especially the surrounding soil matrix (Alaoui *et al.,* 2011). Water transfer between preferential flow paths and the surrounding soil matrix leads to an intensive spatial variation of SWC (Beven & Germann, 1982). Water transfer influenced by the properties of preferential flow paths, the surrounding soil matrix, and preferential flow paths and the surrounding soil matrix interface differ depending on the soil texture. Jarvis *et al.* (2007) stated that the soil water transfer between preferential flow paths and the surrounding soil matrix was higher in coarse soils with high organic matter. Backnäs *et al.* (2012) reported that water transfer was stronger between preferential flow paths formed by coarse grains, plant roots, and the surrounding soil matrix than that between preferential flow paths along stone surfaces and the surrounding soil matrix. Compared with the preferential flow paths, the surrounding soil matrix that stored more capillary water was compacted. Soil water in the surrounding soil matrix was not easily transferred to the surrounding environment. In our study, fine plant roots in the surrounding soil matrix made up approximately 50% of the total fine plant roots. Soil water conservation by plant roots was more evident in the surrounding soil matrix. Studies have shown that the soil organic carbon and microbial biomass is rich in preferential flow paths (Backnäs *et al.,* 2012) and that soil biota activity increases in these areas, whereas such activity was not evident in the surrounding soil matrix.

The SWC observed from certain soil layers decreased after the field dye-tracing experiments in our study. Our field dye-tracing experiments were conducted during a heavy rain season, which resulted in increased soil water flow through preferential flow paths and caused asphyxiation and death of the fine plant roots. Clusters of fine plant roots were in some cases observed along or at the end of the coarse plant roots, and the response areas had high organic nutrients and water uptake. The surrounding soil matrix is usually treated as a coarse aggregate, which promotes more water transfer under heavy rain conditions. Fine plant roots have high decay and emission rates, and clusters might soak up water during the rainy season and contribute to decayed flow paths (Ghestem *et al.,* 2011). Our results implied that the average value of the maximum dye infiltration depth into soil profiles in all of the experimental plots negatively was correlated with the total root length density. The average value of the maximum dye infiltration depth into soil profiles in plots 1, 3, and 5 was higher than in plots 2, 4, and 6, but there was a higher total root length density in plots 2, 4, and 6 than in plots 1, 3, and 5. It is possible that the effects of the root length density depended on the plant species, plant root characteristics and morphology, plant root distribution location in the soils, plant root turnover rates, and soil properties (Ola *et al.,* 2015). These combined factors alter the soil hydrological processes. Our study site was conducted in stony soils of rocky mountainous areas rich in rock fragments. The study site plant roots were usually displaced on the rock fragments surface and in the gaps among the rock fragments in stony soils. It is well known that a dynamic interphase between rock fragments and the surrounding fine earth results in distinct preferential flow properties and that the interphase can have high macroporosity. Rock-to-rock contact increases with increasing rock fragments content. As the rock fragments content increases, there are more continuous preferential flow paths or increased macropore flow or more interphase between rock fragments and the surrounding fine earth (Zhou *et al.,* 2011). Thus, we concluded that preferential flow paths at the study site formed by the interface or cracks between rock fragments and the surrounding fine earth were more evident than that formed by fine plant roots.

CONCLUSIONS

Our study highlighted that preferential flow paths could have strong effects on soil water flow and fine plant root distribution. The following conclusions emerged: First, fine plant roots in preferential flow paths decreased with soil depth and was mostly recorded in the upper soil layers to a depth of 20 cm for all experimental plots. The root length density of the preferential flow paths made up at least 50% of the total root length density at each soil depth. Second, preferential flow effects were most apparent on soil water flow at the 0–20-cm soil depth compared with the other depths (20–40 and 40–60 cm). Third, positive correlations between fine plant roots and changes in the soil water content were observed. Thus, important preferential flow functions should be considered when assessing studies of land degradation in addition to overland flow and surface soil erosion.

ACKNOWLEDGEMENTS

This research was supported by the National Natural Science Foundation of China (41271044) and the Fundamental Research Funds for the Central Universities (2015ZCQ-BH-01). The authors would like to thank Bingpeng Qu,

Yong Liu, and Jingping Tan for their assistance of field work and laboratory analysis. Authors were also grateful to reviewers and editors for their comments and suggestions.

REFERENCES

Alanís N, Hernández-Madrigal VM, Cerdà A, Muñoz-Rojas M, Zavala LM, Jordán A. 2016. Spatial gradients of intensity and persistence of soil water repellency under different forest types in Central Mexico: spatial gradients of soil water repellency in Mexican forests. *Land Degradation & Development*. DOI: 10.1002/ldr.2544.

Alaoui A, Caduff U, Gerke HH, Weingartner R. 2011. Preferential flow effects on infiltration and runoff in grassland and forest soils. *Vadose Zone Journal* **10**: 367–377. DOI: 10.2136/vzj2010.0076.

Alonso-Sarría F, Martínez-Hernández C, Romero-Díaz A, Cánovas-García F, Gomariz-Castillo F. 2016. Main environmental features leading to recent land abandonment in Murcia region (Southeast Spain). *Land Degradation & Development* **27**(3): 654–670. DOI: 10.1002/ldr.2447.

Backnäs S, Laine-Kaulio H, Kløve B. 2012. Phosphorus forms and related soil chemistry in preferential flowpaths and the soil matrix of a forested podzolic till soil profile. *Geoderma* **189-190**: 50–64. DOI: 10.1016/j.geoderma.2012.04.016.

Banaszuk P, Krasowska M, Kamocki A. 2013. Transport of contaminants in agricultural catchments during snowmelt: buffer strips vs. preferential flow paths. *Ecohydrology & Hydrobiology* **13**: 31–40. DOI: 10.1016/j.ecohyd.2013.03.005.

Bargués Tobella A, Reese H, Almaw A, Bayala J, Malmer A, Laudon H, Llstedt U. 2014. The effect of trees on preferential flow and soil infiltrability in an agroforestry parkland in semiarid Burkina Faso. *Water Resources Research* **50**(4): 3342–3354. DOI: 10.1002/2013WR015197.

Bengough AG. 2012. Water dynamic of the root zone: rhizosphere biophysics and its control on soil hydrology. *Vadose Zone Jounal* **11**(2). DOI: 10.2136/vzj2011.0111.

Beniston JW, Lal R, Mercer KL. 2016. Assessing and managing soil quality for urban agriculture in a degraded vacant lot soil. *Land Degradation & Development* **27**(4): 996–1006. DOI: 10.1002/ldr.2342.

Benito Rueda E, Rodríguez-Alleres M, Teijeiro EV. 2016. Environmental factors governing soil water repellency dynamics in a *Pinus pinaster* plantation in NW Spain. *Land Degradation & Development* **27**(3): 719–728. DOI: 10.1002/ldr.2370.

Beven K, Germann P. 1982. Macropores and water flow in soils. *Water Resources Reearch* **18**: 1311–1325. DOI:10.1029/WR018i005p01311.

Beven K, Germann P. 2013. Macropores and water flow in soils revisited. *Water Resources Research* **49**(6): 3071–3092. DOI: 10.1002/wrcr.20156.

Blunt MJ, Bijeljic B, Dong H, Gharbi O, Iglauer S, Mostaghimi P, Paluszny A, Pentland C. 2013. Pore-scale imaging and modelling. *Advances in Water Resources* **51**: 197–216. DOI: 10.1016/j.advwatres.2012.03.003.

Bochet E. 2015. The fate of seeds in the soil: a review of the influence of overland flow on seed removal and its consequences for the vegetation of arid and semiarid patchy ecosystems. *SOIL* **1**: 131–146. DOI: 10.5194/soil-1-131-2015.

Bodí MB, Doerr SH, Cerdà A, Mataix-Solera J. 2012. Hydrological effects of a layer of vegetation ash on underlying wettable and water repellent soils. *Geoderma* **191**: 14–23. DOI: 10.1016/j.geoderma.2012.01.006.

Bodí MB, Muñoz-Santa I, Armero C, Doerr SH, Mataix-Solera J, Cerdà A. 2013. Spatial and temporal variations of water repellency and probability of its occurrence in calcareous Mediterranean rangeland soils affected by fires. *Catena* **108**: 14–24. DOI: 10.1016/j.catena.2012.04.002.

Bodner G, Leitner D, Kaul HP. 2014. Coarse and fine root plants affect pore size distributions differently. *Plant & Soil* **380**: 133–151. DOI: 10.1007/s11104-014-2079-8.

Bogner C, Gaul D, Kolb A, Schmiedinger I, Huwe B. 2010. Investigating flow mechanisms in a forest soil by mixed-effects modelling. *European Journal of Soil Science* **61**: 1079–1090. DOI: 10.1111/j.1365-2389.2010.01300.x.

Brevik EC, Cerdà A, Mataix-Solera J, Pereg L, Quinton JN, Six J, Van Oost K. 2015. The interdisciplinary nature of *SOIL*. *SOIL* **1**: 117–129. DOI: 10.5194/soil-1-117-2015.

Cai Z, Ofterdinger U. 2016. Analysis of groundwater-level response to rainfall and estimation of annual recharge in fractured hard rock aquifers, NW Ireland. *Journal of Hydrology* **535**: 71–84. DOI: 10.1016/j.jhydrol.2016.01.066.

Ceccon C, Panzacchi P, Scandellari F, Prandi L, Ventura M, Russo B, Millard P, Tagliavini M. 2011. Spatial and temporal effects of soil temperature and moisture and the relation to fine root density on root and soil respiration in a mature apple orchard. *Plant & Soil* **342**: 195–206. DOI: 10.1007/s11104-010-0684-8.

Cerdà A. 1996. Seasonal variability of infiltration rates under contrasting slope conditions in Southeast Spain. *Geoderma* **69**: 217–232. DOI: 10.1016/0016-7061(95)00062-3.

Cerdà A. 1998a. The influence of aspect and vegetation on seasonal changes in erosion under rainfall simulation on a clay soil in Spain. *Canadian Journal of Soil Science* **78**: 321–330. DOI: 10.4141/S97-060.

Cerdà A. 1998b. Effect of climate on surface flow along a climatological gradient in Israel. A field rainfall simulation approach. *Journal of Arid Environments* **38**: 145–159. DOI: 10.1006/jare.1997.0342.

Cerdà A. 1998c. Relationship between climate and soil hydrological and erosional characteristics along climatic gradients in Mediterranean limestone areas. *Geomorphology* **25**: 123–134. DOI: 10.1016/S0169-555X(98)00033-6.

Cerdà A. 1998d. Changes in overland flow and infiltration after a rangeland fire in a Mediterranean scrubland. *Hydrological Processes* **12**: 1031–1042. DOI: 10.1002/(SICI)1099-1085(19980615)12:7<1031::AID-HYP636>3.0.CO;2-V.

Cerdà A. 1999. Seasonal and spatial variations in infiltration rates in badland surfaces under Mediterranean climatic conditions. *Water Resources Research* **35**(1): 319–328. DOI: 10.1029/98WR01659.

Cerdà A. 2001. Effects of rock fragment cover on soil infiltration, interrill runoff and erosion. *European Journal of Soil Science* **52**: 59–68. DOI: 10.1046/j.1365-2389.2001.00354.x.

Cerdà A, Doerr SH. 2007. Soil wettability, runoff and erodibility of major dry-Mediterranean land use types on calcareous soils. *Hydrological Processes* **21**: 2325–2336. DOI: 10.1002/hyp.6755.

Cerdà A, Jurgensen MF. 2008. The influence of ants on soil and water losses from an orange orchard in Eastern Spain. *Journal of Applied Entomology* **132**(4): 306–314. DOI: 10.1111/j.1439-0418.2008.01267.x.

Cerdà A, Juergensen MF, Bodí MB. 2009. Effects of ants on water and soil losses from organically-managed citrus orchards in Eastern Spain. *Biologia* **64**: 527–531. DOI: 10.2478/s11756-009-0114-7.

Cerdà A, González-Pelayo Ó, Giménez-Morera A, Jordán A, Pereira P, Novara A, Brevik EC, Prosdocimi M, Mahmoodabadi M, Keesstra S, Orenes FG, Ritsema CG. 2016. Use of barley straw residues to avoid high erosion and runoff rates on persimmon plantations in Eastern Spain under low frequency-high magnitude simulated rainfall events. *Soil Research* **54**: 154–165. DOI: 10.1071/SR15092.

Chen G, Weil RR. 2010. Penetration of cover crop roots through compacted soils. *Plant & Soil* **331**: 31–43. DOI:10.1007/s11104-009-0223-7.

Coppola A, Comegna A, Dragonetti G, Gerke HH, Basile A. 2015. Simulated Preferential Water Flow and Solute Transport in Shrinking Soils. *Vadose Zone Journal* **14**(9). DOI: 10.2136/vzj2015.02.0021.

De Boever M, Gabriels D, Ouessar M, Cornelis W. 2014. Influence of acacia trees on near-surface soil hydraulic properties in arid Tunisia. *Land Degradation & Development* . DOI: 10.1002/ldr.2302.

Duncan MJ, Srinivasan MS, McMillan H. 2016. Field measurement of groundwater recharge under irrigation in Canterbury, New Zealand, using drainage lysimeters. *Agricultural Water Management* **166**: 17–32. DOI: 10.1016/j.agwat.2015.12.002.

DuPont ST, Beniston J, Glover JD, Hodson A, Culman SW, Lal R, Ferris H. 2014. Root traits and soil properties in harvested perennial grassland, annual wheat, and never-tilled annual wheat. *Plant & Soil* **381**: 405–420. DOI: 10.1007/s11104-014-2145-2.

Ferchaud F, Vitte G, Bornet F, Strullu L, Mary B. 2015. Soil water uptake and root distribution of different perennial and annual bioenergy crops. *Plant & Soil* **388**: 307–322. DOI: 10.1007/s11104-014-2335-y.

Finér L, Messier C, Granpré L. 1997. Fine-root dynamics in mixed boreal conifer –broad-leafed forest stands at different successional stages after fire. *Canadian Journal of Forest Research* **27**: 304–314. DOI:10.1139/x96-170.

Finér L, Ohashi M, Noguchi K, Hirano Y. 2011. Fine root production and turnover in forest ecosystems in relation to stand and environmental characteristics. *Forest Ecology & Management* **262**: 2008–2023. DOI: 10.1016/j.foreco.2011.08.042.

Ghestem M, Sidle RC, Stokes A. 2011. The influence of plant root systems on subsurface flow: implications for slope stability. *BioScience* **61**: 869–879. DOI: 10.1525/bio.2011.61.11.6.

Glab T. 2013. Impact of soil compaction on root development and yield of meadow-grass. *International Agrophysics* **27**(1): 7–13. DOI: 10.2478/v10247-012-0062-2.

Goebel MO, Bachmann JBA, Reichstein M, Janssens IA, Guggenberger G. 2011. Soil water repellency and its implications for organic matter decomposition-is there a link to extreme climatic events? *Global Change Biology* **17**: 2640–2656. DOI: 10.1111/j.1365-2486.2011.02414.x.

Granged AJ, Jordán A, Zavala LM, Bárcenas G. 2011. Fire-induced changes in soil water repellency increased fingered flow and runoff rates following the 2004 Huelva wildfire. *Hydrological Processes* **25**: 1614–1629. DOI: 10.1002/hyp.7923.

Haghighi F, Gorji M, Shorafa M. 2010. A study of the effects of land use changes on soil physical properties and organic matter. *Land Degradation & Development* **21**(5): 496–502. DOI: 10.1002/ldr.999.

Han E, Kautz T, Perkons U, Lüsebrink M, Pude R, Köpke U. 2015. Quantification of soil biopore density after perennial fodder cropping. *Plant & Soil* **394**: 73–85. DOI: 10.1007/s11104-015-2488-3.

Hanson DL, Steenhuis TS, Walter MF, Boll J. 2004. Effects of soil degradation and management practices on the surface water dynamics in the Talgua River watershed in Honduras. *Land Degradation & Development* **15**(4): 367–381. DOI: 10.1002/ldr.603.

Harkel MJT, Boxel JHV, Verstraten JM. 1998. Water and solute fluxes in dry coastal dune grasslands: the effects of grazing and increased nitrogen deposition. *Plant & Soil* **202**(1): 1–13. DOI: 10.1023/A:1004336520844.

Hewelke E, Szatylowicz J, Gnatowski T, Oleszczuk R. 2016. Effects of soil water repellency on moisture patterns in a degraded sapric Histosol. *Land Degradation & Development* **27**(4): 955–964. DOI: 10.1002/ldr.2305.

Hlaváčiková H, Novák V, Holko L. 2015. On the role of rock fragments and initial soil water content in the potential subsurface runoff formation. *Journal of Hydrology and Hydromechanics* **63**(1): 71–81. DOI: 10.1515/johh-2015-0002.

Hu B, Han CL, Jia Y, Zhao ZH, Li FM, Siddique KHM. 2013. Visualization of the three-dimensional water-flow paths in calcareous soil using iodide water tracer. *Geoderma* **200-201**: 85–89. DOI: 10.1016/j.geoderma.2013.01.009.

Jarvis NJ. 2007. A review of non-equilibrium water flow and solute transport in soil macropores: principles, controlling factors and consequences for water quality. *European Journal of Soil Science* **58**(3): 523-546. DOI: 10.1111/j.1365-2389.2007.00915.x.

Jarvis NJ, Larsbo M, Roulier S, Lindahl A, Persson L. 2007. The role of soil properties in regulating non-equilibrium macropore flow and solute transport in agricultural topsoils. *European Journal of Soil Science* **58**: 282–292. DOI: 10.1111/j.1365-2389.2006.00837.x.

Jarvis NJ, Moeys J, Koestel J, Hollis JM. 2012. Preferential flow in a pedological perspective. *In*: *Hydropedology*. pp: 75-120. DOI: 10.1016/B978-0-12-386941-8.00003-4.

Jiang XJ, Liu XE, Wang EH, Li XG, Sun R, Shi WJ. 2015. Effects of tillage pan on soil water distribution in alfalfa-corn crop rotation systems using a dye tracer and geostatistical methods. *Soil & Tillage Research* **150**: 68–77. DOI: 10.1016/j.still.2015.01.009.

Jomaa S, Barry DA, Heng BCP, Brovelli A, Sander GC, Parlange JY. 2012. Influence of rock fragment coverage on soil erosion and hydrological response: laboratory flume experiments and modeling. *Water Resources Research* **48**: W05535. DOI: 10.1029/2011WR011255.

Jordán A, Matínez-Zavala LM, Bellinfante N. 2008. Heterogeneity in soil hydrological response from different land cover types in southern Spain. *Catena* **74**: 137–143. DOI: 10.1016/j.catena.2008.03.015.

Jørgensen PR, Hoffmann M, Kistrup JP, Bryde C, Bossi R, Villholth KG. 2002. Preferential flow and pesticide transport in a clay-rich till: field, laboratory, and modeling analysis. *Water Resources Research* **38**: 1246–1261. DOI: 10.1029/2001WR000494.

Katuwal S, Moldrup P, Lamandé M, Tuller M, de Jonge LW. 2015a. Effects of CT number derived matrix density on preferential flow and transport in a macroporous agricultural soil. *Vadose Zone Journal* **14**(7). DOI: 10.2136/vzj2015.01.0002.

Katuwal S, Norgaard T, Moldrup P, Lamandé M, Wildenschild D, de Jonge LW. 2015b. Linking air and water transport in intact soils to macropore characteristics inferred from X-ray computed tomography. *Geoderma* **237-238**: 9–20. DOI: 10.1016/j.geoderma.2014.08.006.

Keesstra SD, Bouma J, Wallinga J, Tittonell P, Smith P, Cerdà A, Montanarella L, Quinton JN, Pachepsky Y, van der Putten WH, Bardgett RD, Moolenaar S, Mol G, Jansen B, Fresco LO. 2016a. The significance of soils and soil science towards realization of the United Nations Sustainable Development Goals. *SOIL* **2**: 111–128. DOI: 10.5194/soil-2-111-2016.

Keesstra SD, Pereira P, Novara A, Brevik EC, Azorin-Molina C, Parras-Alcántara L, Jordán A, Cerdà A. 2016b. Effects of soil management techniques on soil water erosion in apricot orchards. *Science of the Total Environment* **551-552**: 357–366. DOI: 10.1016/j.scitotenv.2016.01.182.

Kramers G, Richards KG, Holden NM. 2009. Assessing the potential for the occurrence and character of preferential flow in three Irish grassland soils using image analysis. *Geoderma* **15**: 362–371. DOI: 10.1016/j.geoderma.2009.08.021.

Krounbi L, Lazarovitch N. 2011. Soil hydraulic properties affecting root water uptake. In Encyclopedia of agrophysics, Gliński J, Horabik J, Lipiec J (eds). Springer Dordrecht: Heidelberg; 748–754. DOI: 10.1007/978-90-481-3585-1_149.

Larsbo M, Koestel J, Jarvis N. 2014a. Controls of macropore network characteristics on preferential solute transport. *Hydrology and Earth System Sciences Discussions* **11**: 9551–9588. DOI:10.5194/hessd-11-9551-2014.

Larsbo M, Koestel J, Jarvis N. 2014b. Relations between macropore network characteristics and the degree of preferential solute transport. *Hydrology and Earth System Sciences* **18**: 5255–5269. DOI: 10.5194/hess-18-5255-2014.

Leh M, Bajwa S, Chaubey I. 2013. Impact of land use change on erosion risk: an integrated remote sensing geographic information system and modeling methodology. *Land Degradation & Development* **24**(5): 409–421. DOI: 10.1002/ldr.1137.

León J, Bodí MB, Cerdà A, Badía D. 2013. The contrasted response of ash to wetting. The effects of ash type, thickness and rainfall events. *Geoderma* **209-210**: 143–152. DOI: 10.1016/j.geoderma.2013.06.018.

Liu Z, Yao Z, Huang H, Wu S, Liu G. 2014. Land use and climate changes and their impacts on runoff in the Yarlung Zangbo River basin, China. *Land Degradation & Development* **25**: 203–215. DOI: 10.1002/ldr.1159.

Malvar MC, Prats SA, Nunes JP, Keizer JJ. 2016. Soil water repellency severity and its spatio-temporal variation in burnt eucalypt plantations in north-central Portugal. *Land Degradation & Development* **27**(5): 1463–1478. DOI: 10.1002/ldr.2450.

Marchamalo M, Hooke JM, Sandercock PJ. 2016. Flow and sediment connectivity in semi-arid landscapes in SE Spain: patterns and controls. *Land Degradation & Development* **27**(4): 1032–1044. DOI:10.1002/ldr.2352.

Mardhiah U, Caruso T, Gurnell A, Rillig MC. 2016. Arbuscular mycorrhizal fungal hyphae reduce soil erosion by surface Water flow in a greenhouse experiment. *Applied Soil Ecology* **99**: 137–140. DOI: 10.1016/j.apsoil.2015.11.027.

Merdun H, Meral R, Demirkiran AR. 2008. Effect of the initial soil moisture content on the spatial distribution of the water retention. *Eurasian Soil Science* **41**(10): 1098–1106. DOI: 10.1134/S1064229308100128.

Mossadeghi-Björklund M, Arvidsson J, Keller T, Koestel J, Lamandé M, Larsbo M, Jarvis N. 2016. Effects of subsoil compaction on hydraulic properties and preferential flow in a Swedish clay soil. *Soil & Tillage Research* **156**: 91–98. DOI: 10.1016/j.still.2015.09.013.

Naveed M, Moldrup P, Schaap M, Tuller M, Kulkarni R, Vögel HJ, Wollesen de Jonge L. 2015. Macropore flow at the field scale: predictive performance of empirical models and X-ray CT analyzed macropore characteristics. *Hydrology and Earth System Sciences Discussions* **12**: 12089–12120. DOI: 10.5194/hessd-12-12089-2015.

Ni J, Luo DH, Xia J, Zhang ZH, Hu G. 2015. Vegetation in karst terrain of southwestern China allocates more biomass to roots. *Solid Earth* **6**: 799–810. DOI: 10.5194/sed-7-1209-2015.

Nimmo JR. 2012. Preferential flow occurs in unsaturated conditions. *Hydrological Processes* **26**(5): 786–789. DOI: 10.1002/hyp.8380.

Nocita M, Stevens A, Noon C, van Wesemael B. 2013. Prediction of soil organic carbon for different levels of soil moisture using Vis-NIR spectroscopy. *Geoderma* **199**: 37–42. DOI: 10.1016/j.geoderma.2012.07.020.

Noguchi S, Tsuboyama Y, Sidle RC, Hosoda I. 1997. Spatially distributed morphological characteristics of macropores in forest soils of Hitachi Ohta Experimental Watershed, Japan. *Journal of Forest Research* **2**(4): 207–215. DOI: 10.1007/BF02348317.

Nosalewicz A, Lipiec J. 2014. The effect of compacted soil layers on vertical root distribution and water uptake by wheat. *Plant & Soil* **375**: 229–240. DOI: 10.1007/s11104-013-1961-0.

Ola A, Dodd IC, Quinton JN. 2015. Can we manipulate root system architecture to control soil erosion? *SOIL* **1**: 603–612. DOI: 10.5194/soild-2-265-2015.

Pereira P, Gimeìnez-Morera A, Novara A, Keesstra S, Jordán A, Masto RE, Brevik E, Azorin-Molina C, Cerdà A. 2015. The impact of road and railway embankments on runoff and soil erosion in eastern Spain. *Hydrology and Earth System Sciences Discussions* **12**: 12947–12985. DOI: 10.5194/hessd-12-12947-2015.

Perkins KS, Nimmo JR, Rose CE, Coupe RH. 2011. Field tracer investigation of unsaturated zone flow paths and mechanisms in agricultural soils of northwestern Mississippi, USA. *Journal of Hydrology* **396**: 1–11. DOI: 10.1016/j.jhydrol.2010.09.009.

Perkons U, Kautz T, Uteau D, Peth S, Geier V, Thomas K, Lütke Holz K, Athmann M, Pude R, Köpke U. 2014. Root-length densities of various annual crops following crops with contrasting root systems. *Soil & Tillage Research* **137**: 50–57. DOI: 10.1016/j.still.2013.11.005.

Raizada A, Jayaprakash J, Rathore AC, Tomar JMS. 2013. Distribution of fine root biomass of fruit and forest tree species raised on old river bed lands in the north west Himalaya. *Tropical Ecology* **54**(2): 251–261.

Reading LP, Baumgartl T, Bristow KL, Lockington DA. 2012. Hydraulic conductivity increases in a sodic clay soil in response to gypsum applications: impacts of bulk density and cation exchange. *Soil Science* **177**(3): 165–171. DOI: 10.1097/SS.0b013e3182408f4f.

Rodríguez-Alleres M, Benito E. 2011. Spatial and temporal variability of surface water repellency in sandy loam soils of NW Spain under *Pinus pinaster* and *Eucalyptus globulus* plantations. *Hydrological Processes* **25**: 3649–3658. DOI: 10.1002/hyp.8091.

Rodríguez-Alleres M, Varela ME, Benito E. 2012. Natural severity of water repellency in pine forest soils from NW Spain and influence of wildfire severity on its persistence. *Geoderma* **191**: 125–131. DOI: 10.1016/j.geoderma.2012.02.006.

Roy M, McDonald LM. 2015. Metal uptake in plants and health risk assessment in metal-contaminated smelter soils. *Land Degradation & Development* **26**: 785–792. DOI: 10.1002/ldr.2237.

Ruark GA, Bockheim JG. 1987. Below-ground biomass of 10-, 20-, and 32-year-old *Populus tremuloides* in Wisconsin. *Pedobiologia* **30**: 207–217.

Sammartino S, Michel E, Capowiez Y. 2012. A novel method to visualize and characterize preferential flow in undisturbed soil cores by using multislice helical CT. *Vadose Zone Journal* **11**(1). DOI: 10.2136/vzj2011.0100.

Sanders EC, Abou Najm MR, Mohtar RH, Kladivko E, Schulze D. 2012. Field method for separating the contribution of surface-connected preferential flow pathways from flow through the soil matrix. *Water Resources Research* **48**: 4534–4542. DOI: 10.1029/2011WR011103.

Santos JM, Verheijen FGA, Wahren FT, Wahren A, Feger KH, Bernard-Jannin L, Rial-Rivas ME, Keizer JJ, Nunes JP. 2016. Soil water repellency dynamics in pine and eucalypt plantations in Portugal—a high-resolution time series. *Land Degradation & Development* **27**(5): 1334–1343. DOI:10.1002/ldr.2251.

Shein EV. 2010. Soil hydrology: stages of development, current state, and nearest prospects. *Eurasian Soil Science* **43**(2): 158–167. DOI: 10.1134/S1064229310020055.

Shinohara Y, Otsuki K. 2015. Comparisons of soil-water content between a Moso bamboo (*Phyllostachys pubescens*) forest and an evergreen broadleaved forest in western Japan. *Plant Species Biology* **30**: 96–103. DOI: 10.1111/1442-1984.12076.

Singh YP, Nayak AK, Sharma DK, Singh G, Mishra VK, Singh D. 2015. Evaluation of *Jatropha curcas* genotypes for rehabilitation of degraded sodic lands. *Land Degradation & Development* **26**(5): 510–520. DOI: 10.1002/ldr.2398.

Steenhuis TS, Richard TL, Parlange MB, Aburime SO, Geohring LD, Parlange JY. 1988. Preferential flow influences on drainage of shallow sloping soils. *Agricultural Water Management* **14**: 137–151. DOI: 10.1016/0378-3774(88)90069-8.

Tracy SR, Black CR, Roberts JA, Mooney SJ. 2011. Soil compaction: a review of past and present techniques for investigating effects on root growth. *Journal of the Science of Food & Agriculture* **91**: 1528–1537. DOI: 10.1002/jsfa.4424.

Tracy SR, Black CR, Roberts JA, Mooney SJ. 2013. Exploring the interacting effect of soil texture and bulk density on root system development in tomato (*Solanum lycopersicum* L.) *Environmental & Experimental Botany* **91**: 38–47. DOI: 10.1016/j.envexpbot.2013.03.003.

Vannoppen W, Vanmaerckea M, De Baets S, Poesen J. 2015. A review of the mechanical effects of plant roots on concentrated flow erosion rates. *Earth-Science Reviews* **150**: 666–678. DOI: 10.1016/j.earscirev.2015.08.011.

Wang Y, Fan J, Cao L, Liang Y. 2016. Infiltration and runoff generation under various cropping patterns in the red soil region of China. *Land Degradation & Development* **27**(1): 83–91. DOI: 10.1002/ldr.2460.

Wildemeersch JCJ, Garba M, Sabiou M, Sleutel S, Cornelis W. 2015. The effect of water and soil conservation (WSC) on the soil chemical biological, and physical quality of a plinthosol in Niger. *Land Degradation & Development* **26**(7): 774–784. DOI: 10.1002/ldr.2416.

Wu QS, Cao MQ, Zou YN, He XH. 2014. Direct and indirect effects of glomalin, mycorrhizal hyphae, and roots on aggregate stability in rhizosphere of trifoliate orange. *Scientific Reports* **4**: 5823–5830. DOI: 10.1038/srep05823.

Xin P, Yu X, Lua C, Li L. 2016. Effects of macro-pores on water flow in coastal subsurface drainage systems. *Advances in Water Resources* **87**: 56–67. DOI: 10.1016/j.advwatres.2015.11.007.

Yagüe MR, Domingo-Olivé F, Bosch-Serra AD, Poch RM, Boixadera J. 2016. Dairy cattle manure effects on soil quality: porosity, earthworms, aggregates and soil organic carbon fractions. *Land Degradation & Development*. DOI: 10.1002/ldr.2477.

Yan HF, Li K, Ding H, Liao CS, Li XX, Yuan LX, Li CJ. 2011. Root morphological and proteomic responses to growth restriction in maize plants supplied with sufficient N. *Journal of Plant Physiology* **168**(10): 1067–1075. DOI: 10.1016/j.jplph.2010.12.018.

Yavitt JB, Harms KE, Garcia MN, Mirabello MJ, Wright SJ. 2011. Soil fertility and fine root dynamics in response to 4 years of nutrient (N, P, K) fertilization in a lowland tropical moist forest, Panama. *Austral Ecology* **36**: 433–445. DOI: 10.1111/j.1442-9993.2010.02157.x.

Yüksek T, Kurdoğlu O, Yüksek F. 2010. The effects of land use changes and management types on surface soil properties in Kafkasör protected area in Artvin, Turkey. *Land Degradation & Development* **21**(6): 582–590. DOI: 10.1002/ldr.1000.

Zehe E, Graeff T, Morgner M, Bauer A, Bronstert A. 2010. Plot and field scale soil moisture dynamics and subsurface wetness control on runoff generation in a headwater in the Ore Mountains. *Hydrology and Earth System Sciences* **14**: 873–889. DOI: 10.5194/hess-14-873-2010.

Zema DA, Bingner RL, Denisi P, Govers G, Licciardello F, Zimbone SM. 2012. Evaluation of runoff, peak flow and sediment yield for events simulated by the ANNAGNPS model in a Belgian agricultural watershed. *Land Degradation & Development* **23**(3): 205–215. DOI: 10.1002/ldr.1068.

Zhang ZB, Peng X, Wang L, Zhao Q, Lin H. 2013. Temporal changes in shrinkage behavior of two paddy soils under alternative flooding and drying cycles and its consequence on percolation. *Geoderma* **192**: 12–20. DOI: 10.1016/j.geoderma.2012.08.009.

Zhang YH, Niu JZ, Yu XX, Zhu WL, Du XQ. 2015a. Effects of fine root length density and root biomass on soil preferential flow in forest ecosystems. *Forest Systems* **24**(1): e012. DOI: 10.5424/fs/2015241-06048.

Zhang ZB, Peng X, Zhou H, Lin H, Sun H. 2015b. Characterizing preferential flow in cracked paddy soils using computed tomography and breakthrough curve. *Soil & Tillage Research* **146**: 53–65. DOI: 10.1016/j.still.2014.05.016.

Zhang YH, Zhang MX, Niu JZ, Li HL, Xiao R, Zheng HJ, Bechd J. 2016a. Rock fragments and soil hydrological processes: significance and progress. *Catena* **147**: 153–166. DOI: 10.1016/j.catena.2016.07.012.

Zhang YH, Zhang MX, Niu JZ, Zheng HJ. 2016b. The preferential flow of soil: A widespread phenomenon in pedological perspectives. *Eurasian Soil Science* **49**(6): 661–672. DOI: 10.1134/S1064229316060120.

Zhao C, Gao J, Huang Y, Wang G, Zhang M. 2016. Effects of vegetation stems on hydraulics of overland flow under varying water discharges. *Land Degradation & Development* **27**(3): 748–757. DOI: 10.1002/ldr.2423.

Zhou BB, Shao M, Wen MK, Wang QJ, Horton R. 2010. Effects of coal gangue content on water movement and solute transport in a China Loess Plateau soil. *CLEN-Soil, Air, Water* **38**(11): 1031–1038. DOI: 10.1002/clen.201000056.

Zhou BB, Shao MA, Wang QJ, Yang T. 2011. Effects of different rock fragment contents and sizes on solute transport in soil columns. *Vadose Zone Journal* **10**(1): 386–393. DOI: 10.2136/vzj2009.0195.